Supplemental Data

Materials and Methods

In vitro lipid oxidation experiments

For free radical-catalyzed oxidation,10 mg of fatty acids (18:1, 18:2, 18:3, 9-HOO-18:3 and 13-HOO-18:3) were dissolved in 1 mL of diethyl ether and dried in a 50 mL round bottomed flask. Thin film oxidation of neat fatty acids was accomplished by incubation of the open flask at room temperature in the dark for 24 h. Lipids were dissolved in 1.5 ml of methanol and the autoxidation reaction was stopped by adding 3.5 mL of water containing 10 mg of $SnCl_2$ to reduce all peroxides to the corresponding alcohols. After adjusting the pH to 3 with 1M citric acid, the mixture was extracted with diethyl ether. The organic phase was dried and the residue reconstituted in acetonitrile for UPLC-MS/MS analysis.

Thin film oxidation in the dark yields HOO-18:3 exclusively formed by a free radical-catalyzed mechanism. The mol% yield for each isomer is shown in Fig. S2A. The relative isomer distribution of the six possible HOO-18:3 isomers is in well agreement with the isomer distribution (as % of total HOO-18:3) reported in the literature (Frankel, 2005): 9-HOO-18:3 (31%), 10-HOO-18:3 (0%), 12-HOO-18:3 (10%), 13-HOO-18:3 (11%), 15-HOO-18:3 (0%), 16-HOO-18:3 (48%). Note, that the 10- and 15-isomer cannot be formed by free radical catalyzed 18:3 oxidation.

Photosensitized oxidation was performed in the light (350 µmol m^{-2} s^{-1}). Fatty acids (10 mg) were dissolved in 1 ml methanol with or without addition of 0.5% (w/v) BHT. The reaction was started by adding 0.1 mM methylene blue in 3 mL of H_2O. After incubation for 2 h at room temperature, the reaction was stopped by adding 10 mg of $SnCl_2$. Lipids were extracted by solvent extraction as described above.

Photooxidation of 18:3 in the presence of the radical scavenger BHT yields HOO-18:3 isomers that were almost exclusively formed by $^1O_2$. However, even high amounts of BHT cannot completely suppress free radical-catalyzed oxidation of 18:3. The mol% yield for each isomer is shown in Fig. S2C. The relative isomer distribution of the six possible HOO-18:3 isomers is in good agreement with the predicted photooxidation isomer pattern (as % of total HOO-18:3) reported in the literature (Frankel, 2005): 9-HOO-18:3 (20%), 10-HOO-18:3 (20%), 12-HOO-18:3 (20%), 13-HOO-18:3 (20%), 15-HOO-18:3 (20%), 16-HOO-18:3 (20%). Note, that the 10- and 15-isomers are specific $^1O_2$-products of 18:3 oxidation.

The reported literature values for the 18-HOO-18:3 isomer distribution (Frankel, 2005) have been used to calculate the relative contribution of $^1O_2$-, free radical and lipoxygenase mechanisms for total HOO-18:3 formation *in vitro* and *in vivo*. The calculations are in agreement with the results of the *in vitro* $^1O_2$ and free radical model oxidation experiments (Fig S2 C and D).

Calculation of $^1O_2$-product levels: Since the $^1O_2$-oxidation mechanism produces the six theoretically possible isomers with equal abundance, levels of each isomer formed through $^1O_2$-oxidation equals the level of the $^1O_2$-specific 10- or 15-HOO-18:3 isomer, and hence, can be calculated from the known levels of these isomers.

Calculation of free radical-product levels: The 16- HOO-18:3 isomer can be formed through a $^1O_2$ or free radical oxidation mechanism but not through enzymatic mechanisms. Subtraction of the level of 16-HOO-18:3 formed by $^1O_2$ from the total level of 16-HOO-18:3 yields the level of 16-HOO-18:3 formed by free radical oxidation. Since the relative isomer distribution of HOO-18:3 produced by free radical oxidation is known, levels of all HOO-18:3 isomers formed through free radical catalysis can be calculated.

Calculation of 9- and 13-LOX-product levels: The 9- and 13-HOO-18:3 isomers can be produced through lipoxygenases or non-enzymatic oxidation. Subtraction of the level of non-enzymatically formed 9- and 13-HOO-18:3 isomers from the total level of 9- and 13-HOO-18:3 isomers yields the levels of the LOX products.

Analysis of oxidized complex lipids

Lipids were analysed with a Waters Micromass Quattro Premier triple quadrupole mass spectrometer (Milford, MA, USA) in the negative electrospray (ESI) mode with a capillary voltage of 3 kV and positive ESI with a positive capillary voltage of 2.4 kV. The ion source was set at 120°C and N_2 was used as desolvation gas with a flow of 800L/h at 350°C. Argon was used for collision-induced dissociation (flow rate of 0.3 mL/min, 3 x 10^{-3} mBar). The cone voltage and collision energy were optimized for all compounds and selected mass transitions were monitored. For the determination of hydroxy fatty acids, 15-hydroxy-11,13(*Z,E*)-eicosadienoic acid (15-HEDE) was used as internal standard and response factors were determined as described elsewhere (Triantaphylides *et al.*, 2008). For analysis of fragmented fatty acids, sebacic acid was employed as internal standard using response factors determined from the analysis of reference compounds. For the analysis of complex lipids,

(18:0, 18:0)MGDG, (18:0, 18:0)DGDG, (10:0, 10:0, 10:0)TG, (17:0, 17:0)PG, (16:0, 16:0)PI, (17:0, 17:0)PS, (18:0, 18:0)PE and (17:0, 17:0)PC were used as internal standards for each class of compounds. PE and TG species were determined in the positive electrospray mode. In the case of PE $[M+H]^+$ precursor ions and in the case of TG $[M+NH_4^+]^+$ precursor ions were fragmented. All other lipid precursor ions were measured in the negative electrospray mode and the $[M-H]^-$ species were fragmented. Notably, the ionization efficiency may be influenced by the solvent composition and matrix compounds co-eluting from the UPLC column. For instance, water-acetonitrile gradients were found to display a strong dependency of the ionization efficiency on the solvent composition (e.g. the retention time). Therefore, a water-methanol gradient was used that only minimally influenced the ionization efficiency in the chromatographic regions of interest. In addition, the chromatographic separation was optimized to minimize potential ion suppression effects of matrix compounds.

Molecular ions of lipids were fragmented in the collision cell whereby the molecular ion loses the product ions (acyl chains at sn_1, sn_2 and, in the case of TG, sn_3) listed in the table. The loss of the acyl chain from the sn_1 position is the preferred fragmentation process compared to the one from the sn_2 position, however, the fragmentation efficiency is similar for oxidized and non-oxidized acyl chains within one class of compounds. Therefore, for semi-quantitative analysis (assuming a response factor of one for each analyte/internal standard pair), peak areas in the multiple reaction monitoring (MRM) chromatograms of the listed product ions were integrated together and quantitated with respect to the intensities of the product ions of the corresponding internal standards.

Literature cited

Frankel, E.N. (2005) *Lipid oxidation*. Dundee: The Oily Press LTD.

Triantaphylides C, Krischke M, Hoeberichts FA, Ksas B, Gresser G, Havaux M, Van Breusegem F, Mueller MJ (2008) Singlet oxygen is the major reactive oxygen species involved in photooxidative damage to plants. Plant Physiol 148: 960-968

Supplementary Table S1: Mass transitions and conditions for electrospray ionization HPLC-MS/MS analysis.

Compound	Precursor ion *(m/z)*	Product ions *(m/z)*	Cone Voltage (V)	Collision energy (eV)
(18:0, 18:0)MGDG	785.6	283.3	40	26
(18:3, 16:3)MGDG	745.5	277.2, 249.2	40	26
(18:3, 18:3)MGDG	773.5	277.2	40	26
(18:3, OH-16:3)MGDG	761.5	277.2, 265.2	40	26
(16:3, OH-18:3)MGDG	761.5	249.2, 293.2	40	26
(18:3, OH-18:3)MGDG	789.5	277.2, 293.2	40	26
(OH-18:3, OH-16:3)MGDG	777.5	293.2, 265.2	40	26
(OH-18:3, OH-18:3)MGDG	805.5	293.2	40	26
(16:3, ONA)MGDG	639.4	249.2, 171.1	40	26
(18:3, ONA)MGDG	667.4	277.2, 171.1	40	26
(18:3, OHA)MGDG	639.4	277.2, 143.1	40	26
(16:3, AZA)MGDG	655.4	249.2, 187.1	40	26
(18:3, AZA)MGDG	683.4	277.2, 187.1	40	26
(18:3, PIM)MGDG	655.4	277.2, 159.1	40	26
Arabidopside A	773.5	291.2, 263.2	40	26
Arabidopside B	801.5	291.2	40	26
Arabidopside E	1047.5	291.2, 263.2	40	26
Arabidopside G	1075.5	291.2	40	26
(18:0, 18:0)DGDG	947.7	283.3	40	26
(18:3, 16:3)DGDG	907.5	277.2, 249.2	40	26
(18:3, 18:3)DGDG	935.6	277.2	40	26
(18:3, OH-16:3)DGDG	923.5	277.2, 265.2	40	26
(16:3, OH-18:3)DGDG	923.5	249.2, 293.2	40	26
(18:3, OH-18:3)DGDG	951.6	277.2, 293.2	40	26
(OH-18:3, OH-16:3)DGDG	939.5	293.2, 265.2	40	26
(OH-18:3, OH-18:3)DGDG	967.6	293.2	40	26
(16:3, ONA)DGDG	801.4	249.2, 171.1	40	26
(18:3, ONA)DGDG	829.5	277.2, 171.1	40	26
(18:3, OHA)DGDG	801.4	277.2, 143.1	40	26
(16:3, AZA)DGDG	817.4	249.2, 187.1	40	26
(18:3, AZA)DGDG	845.5	277.2, 187.1	40	26
(18:3, PIM)DGDG	817.4	277.2, 159.1	40	26
Arabidopside C	935.5	291.2, 263.2	40	26
Arabidopside D	963.5	291.2	40	26
(17:0, 17:0)PG	749.5	269.2	48	40
(18:3, 16:1)PG	741.5	277.2, 253.2	48	40

(OH-18:3, 16:1)PG	757.5	293.2, 253.2	48	40
(18:3, 16:0)PG	743.5	277.2, 255.2	48	40
(OH-18:3, 16:0)PG	759.5	293.2, 255.2	48	40
(17:0, 17:0)PC	820.5	269.2	40	26
(18:3, 18:2)PC	778.5	277.2, 279.2	40	26
(OH-18:3, 18:2)PC	794.5	293.2, 279.2	40	26
(18:3, 18:3)PC	776.5	277.2	40	26
(OH-18:3, 18:3)PC	792.5	277.2, 293.2	40	26
(18:3, 16:0)PC	754.5	277.2, 255.2	40	26
(OH-18:3, 16:0)PC	770.5	293.2, 255.2	40	26
(16:0, 16:0)PI	809.5	255.2	38	42
(18:3, 16:0)PI	831.5	277.2, 255.2	38	42
(OH-18:3, 16:0)PI	847.5	293.2, 255.2	38	42
(17:0, 17:0)PS	762.5	269.2	40	42
(18:3, 16:0)PS	756.5	277.2, 255.2	40	42
(OH-18:3, 16:0)PS	772.5	293.2, 255.2	40	42
(18:0, 18:0)PE	748.5	607.5	32	22
(18:3, 16:0)PE	714.5	573.5	32	22
(OH-18:3, 16:0)PE	730.5	589.5	32	22
(10:0, 10:0, 10:0)TG	572.4	383.3	32	25
(18:3, 18:3, 18:3)TG	890.7	595.5	32	25
(18:3, 18:3, OH-18:3)TG	906.7	611.5, 595.5	32	25
(18:3, OH-18:3, OH-18:3)TG	922.7	611.5, 627.5	32	25
(18:3, 18:3, 18:2)TG	892.7	595.5, 597.5	32	25
(18:3, OH-18:3, 18:2)TG	908.7	611.5, 613.5, 597.5	32	25
(OH-18:3, OH-18:3, 18:2)TG	924.7	613.5, 627.5	32	25
(18:3, 18:2, 16:0)TG	870.7	597.5, 575.5, 573.5	32	25
(OH-18:3, 18:2, 16:0)TG	886.7	613.5, 575.5, 589.5	32	25
(18:3, 18:3, 16:0)TG	868.7	595.5, 573.5	32	25
(18:3, OH-18:3, 16:0)TG	884.7	611.5, 589.5, 573.5	32	25
(OH-18:3, OH-18:3, 16:0)TG	900.7	627.5, 589.5	32	25
Sebacic acid	201.1	139.1	20	14
OHA	143.1	125.1	20	12
PIM	159.1	97.1	20	14
ONA	171.1	127.1	20	12
AZA	187.1	125.1	20	14
Dihydro-JA	211.2	59.1	19	17
JA	209.2	59.1	19	17
OPDA	291.2	165.1	22	26

15-HEDE	323.1	223.2	26	20
9-HOTE	293.1	171.2	26	20
10-HOTE	293.1	155.2	26	20
12-HOTE	293.1	211.2	26	20
13-HOTE	293.1	195.2	26	20
15-HOTE	293.1	223.2	26	20
16-HOTE	293.1	235.2	26	20

Supplemental Figures

Figure S1

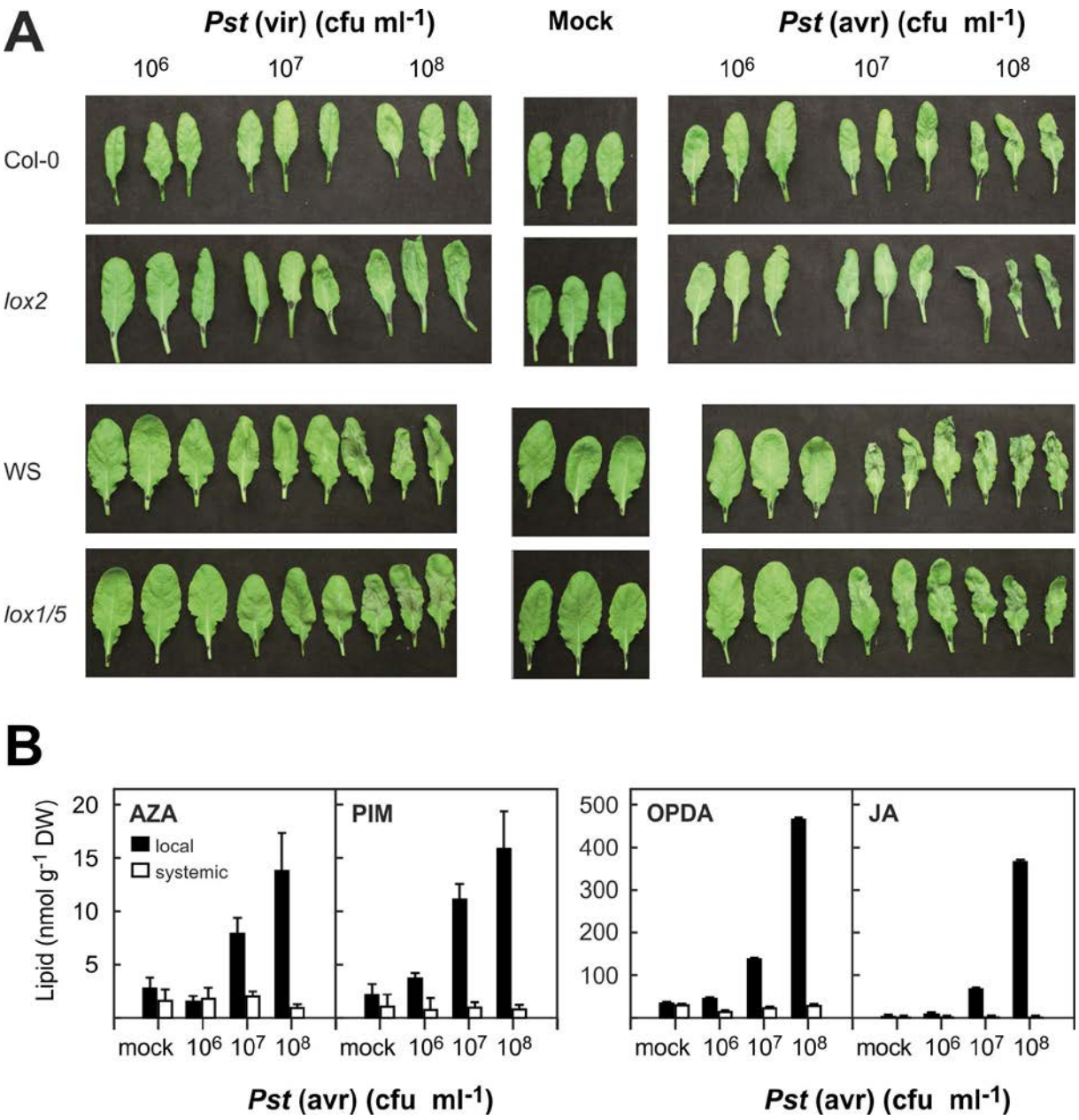

Supplementary Figure S1. Visible leave damage and increased levels of oxidized lipids in local but not in systemic leaves after infection with *Pst*. Leaves were infiltrated with different concentrations of virulent *Pseudomonas syringae* pv. *tomato* (*Pst* DC3000) and avirulent *Pseudomonas syringae* pv. *tomato* (*Pst* DC3000 avrRPM1) in 10 mM $MgSO_4$, respectively, or mock infiltrated with 10 mM $MgSO_4$.

A, photographs of representative leaves 24 h after inoculation.

B, levels of non-enzymatically (AZA and PIM) and enzymatically (OPDA and JA) oxidized lipids in locally infected (black bars) and systemic, non-infected (white bars) leaves of the same plants 24 h after inoculation (means ± SD, n = 5)

Figure S2

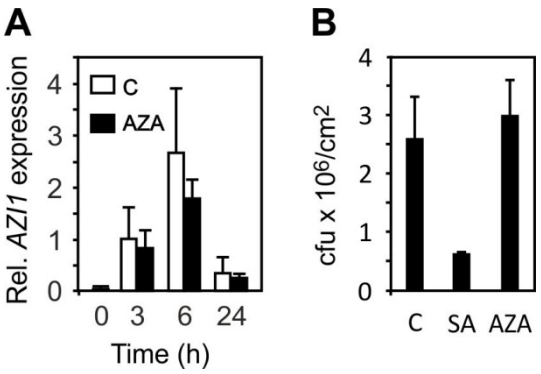

Supplemental Figure S2. Lack of effect of AZA treatment on local defense responses against *P. syringae* DC3000 and expression of *AZI1*.

A, AZA does not induce *AZI1* expression. *AZI1* expression (relative to actin 2/8) in untreated leaves (0 h) or leaves sprayed with 5 mM MES buffer, pH 5.6, (C) or 1 mM AZA in MES buffer (AZA) after 3, 6 and 24 h. Values are means (SEM) of three independent experiments, with relative expression value of AZI1 3 h after buffer treatment was set as 1.

B, salicylic acid, but not AZA treatment, reduces growth of *P. syringae* DC3000. Plants were sprayed with 5 mM MES buffer, pH 5.6, (C), 1 mM sodium salicylate (SA) or 1 mM AZA (AZA) in MES buffer two days before infiltration with *Pst* DC3000 (OD_{600} = 0.005). Pathogen growth was determined three days after infection. Shown are means ± SEM, n=8. The experiment was performed three times with similar results.

Figure S3

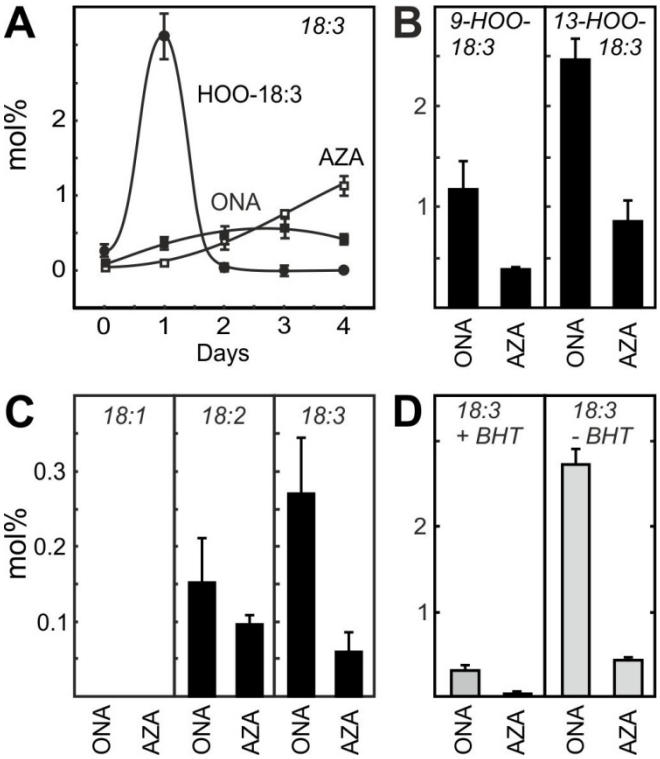

Supplementary Figure S3. Kinetics of singlet oxygen- and free radical-mediated fatty acid oxidation *in vitro*.

A-C, free radical-catalyzed fatty acid oxidation experiments (thin film autoxidation) using the indicated starting molecules were performed and levels of ONA and AZA were determined after different time points (A) or after 24 h (B, C). D, $^1O_2$-mediated oxidation (photooxidation) of 18:3 for 2h: ONA and AZA levels were also determined in the presence or absence of the radical scavenger BHT (c). Shown are means ± SD, n = 3.

Figure S4

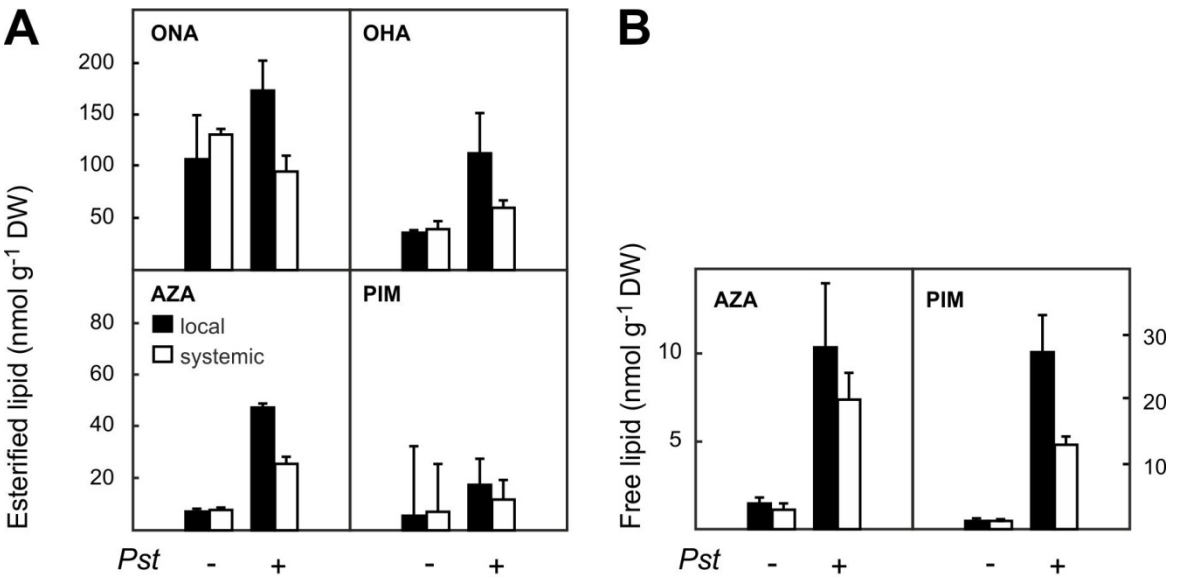

Supplementary Figure S4

Total levels of free and esterified fragmented fatty acids in Arabidopsis WT and *lox2* mutant plants. Levels of fragmented fatty acids in WT (black bars) and *lox2* mutant (white bars) Arabidopsis plants were determined in lipid extracts in free form or after alkaline hydrolysis. A, levels of esterified fragmented fatty acids calculated from the levels in lipid hydrolysates from which levels of free fragmented fatty acids were subtracted. B, levels of free fragmented fatty acids. Shown are means ± SD, n = 3.

Figure S5

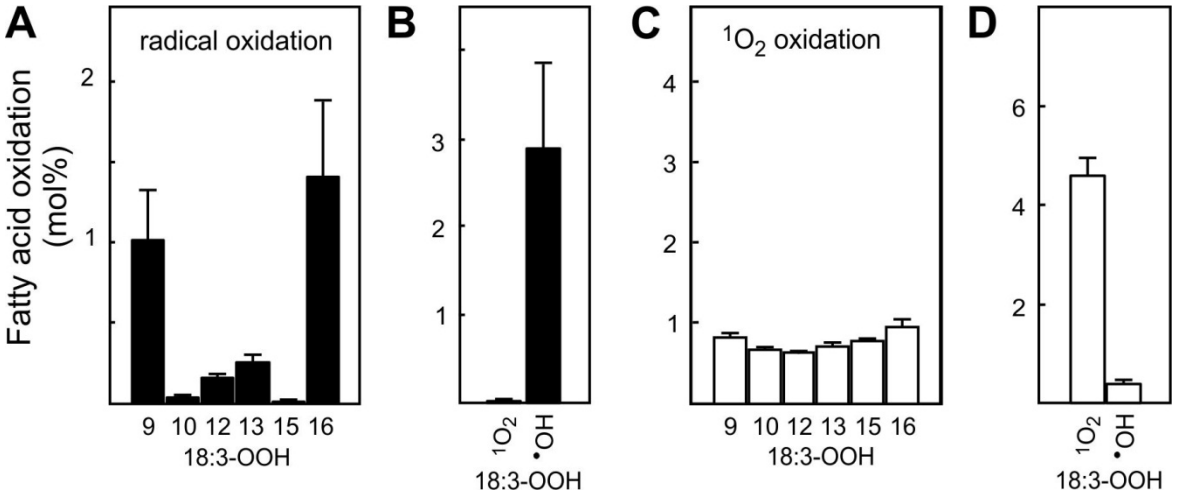

Supplementary Figure S5. Isomer patterns of HOO-18:3 after $^1O_2$ or free radical-catalyzed oxidation of 18:3 *in vitro*. A, isomer pattern of HOO-18:3 determined after free radical-catalyzed oxidation of 18:3, from which, B, the amount of HOO-18:3 formed through the $^1O_2$ and free radical mechanism was calculated (see supplementary material and methods). C, isomer pattern of HOO-18:3 determined after photosensitized oxidation of 18:3 in the presence of the radical scavenger BHT, from which, D, the amount of HOO-18:3 formed through the $^1O_2$ and free radical mechanism was calculated (see supplementary material and methods). The relative yield of different HOO-18:3 isomers (as mol% of total 18:3) obtained from *in vitro* oxidation of 18:3 is shown.

Figure S6

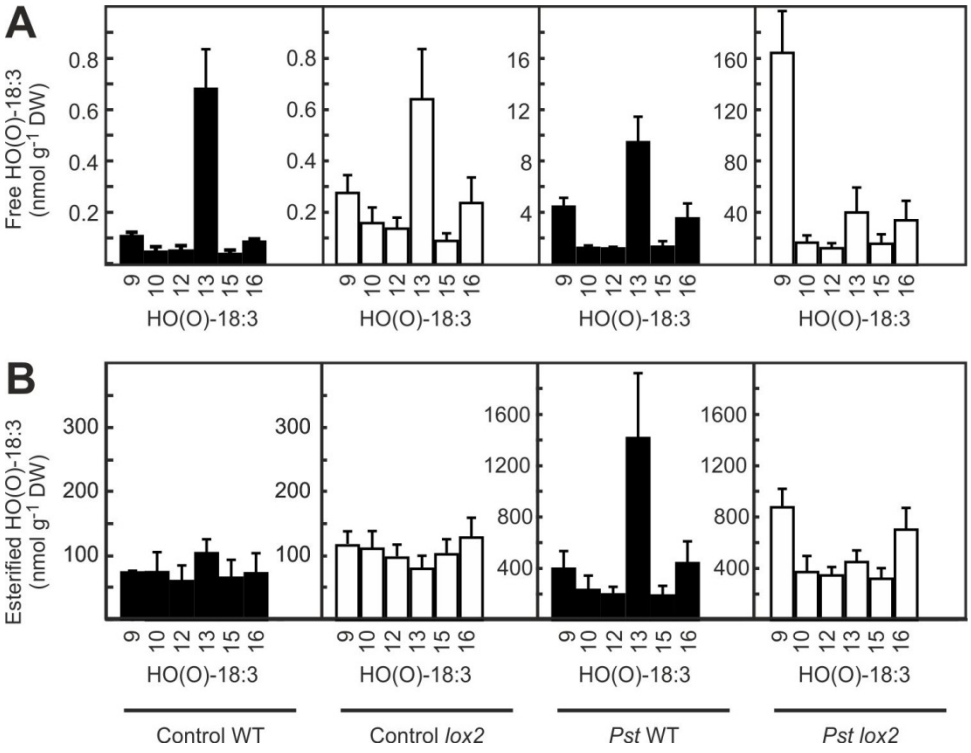

Supplementary Figure S6. Isomer patterns of free and esterified HO(O)-18:3 in *A. thaliana* wild type and *lox2* leaves after infection with avirulent *Pst*.

The isomer pattern of fatty acid peroxides was determined in total lipid extracts from leaves after reduction to the corresponding hydroxy fatty acids by UPLC-MS/MS. HO(O)-18:3 levels were determined 24h after mock (basal) or *Pseudomonas* (*Pst*) infiltration of leaves. An aliquot of the reduced total lipid extract was hydrolyzed to determine levels of total (free and esterified) HO(O)-18:3. Another aliquot was analyzed directly to determine levels of free HO(O)-18:3 (A). Levels of esterified HO(O)-18:3 (B) were calculated by subtracting levels of free HO(O)-18:3 from total HO(O)-18:3 levels. Shown are means ± SD, n = 3.

Figure S7

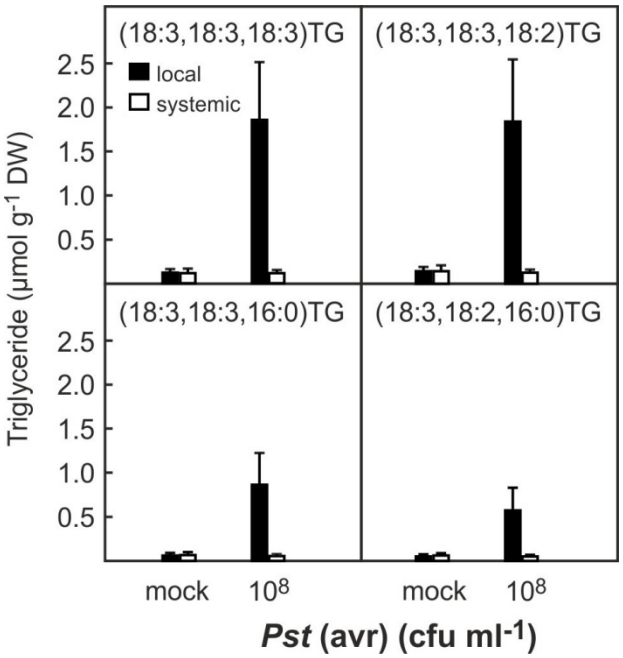

Supplementary Figure S7. Increase of triglyceride levels in local but not in systemic leaves after infection with avirulent *Pst*. Levels of the four most abundant triglycerides in locally infected (black bars) and systemic, non-infected (white bars) leaves of the same plants 24 h after inoculation (means ± SD, n = 5)

Figure S8

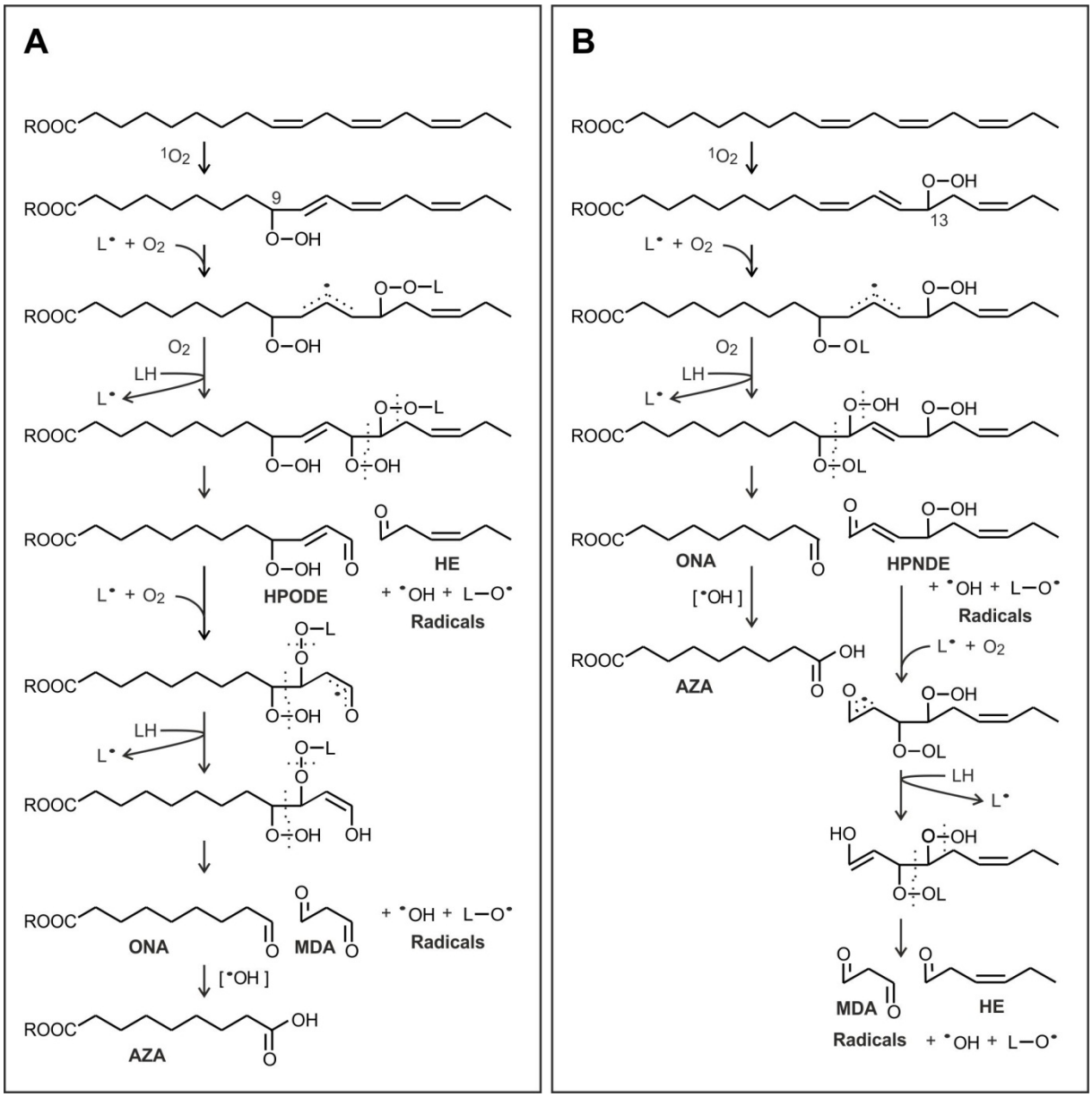

Supplementary Figure S8. Non-enzymatic fragmentation mechanism of 9- and 13-HOO-18:3. In Arabidopsis leaves, a pool of oxidized galactolipids comprising HOO-18:3 is generated by singlet oxygen. Subsequent dimer formation and fragmentation is initiated by free radicals and amplifies the total amount of free radicals. The fragmentation pathway of two out of six possible HOO-18:3 isomers is shown: A, 9-HOO-18:3, and B, 13-HOO-18:3. Abbreviations are: HPODE, 9-hydroperoxy-12-oxo-10-dodecenoate; HE, 2-hexenal; ONA, 9-oxononanoate; MDA, malondialdehyde, AZA, azeleate; HPNDE, 4-hydroperoxy-2,6-nonadienal; L, lipid.